Micro- and ultra-structures of phaeodarian Radiolaria

Takahashi, Kozo
Department of Earth & Planetary Sciences, Graduate School of Sciences, Kyushu University

Hurd, David C
Department of Earth & Planetary Sciences, Graduate School of Sciences, Kyushu University

https://doi.org/10.5109/11810

出版情報：九州大学大学院理学研究院紀要 : Series D, Earth and planetary sciences. 31 (4), pp.137-158, 2007-02-15. Faculty of Science, Kyushu University
バージョン：
権利関係：

Mem. Fac. Sci., Kyushu Univ., Ser. D, Earth & Planet. Sci., Vol. XXXI, No. 4,
pp. 137-158, plates 1-16, February 1, 2007

Micro- and ultra-structures of phaeodarian Radiolaria

Kozo TAKAHASHI* and David C. HURD**

Abstract

SEM and TEM observations of up to x100,000 magnification were performed on the skeletons of phaeodarian Radiolaria mainly acquired by sediment traps. In addition for the sake of comparison, fresh plankton tow specimens were also observed as well as fossil phaeodarians from sediments. The presence of a variety of microstructures is apparent depending on taxa as well as different parts of the skeletons. However, fundamentally porous micro-structures and basic tubular ultra-structures appear to be common in most of the taxa examined. Progressive dissolution of their skeletons can be deciphered when live specimens from a plankton tow and partially dissolved sediment trap samples are compared. Comparative observations on ashed and non-ashed specimens did not show evidence of the presence of organic matter within the phaeodarian skeletal structure.

Keywords: Phaeodaria, Radiolaria, ultra-structure, TEM, porous skeletons, dissolution

1. Introduction

Morphological structures of phaeodarian Radiolaria (Phaeodaria hereafter; TAKAHASHI and ANDERSON, 2002) are complex and vary significantly depending on the taxa. The porosity of the skeletons is partially responsible for their rapid dissolution in the ocean water column and sea-floor. The porous skeletons with higher specific surface areas and water contents appear to be different from those of a more solution resistant counterpart called "polycystine Radiolaria" (Polycystina hereafter; ANDERSON *et al*., 2002) (HURD *et al*. 1981; HURD and TAKAHASHI, 1983; TAKAHASHI *et al*., 1983; TAKAHASHI, 1991).

An overview of phaeodarian morphology is appropriate for formulating descriptive preservation models in a broad range of environments. Together with the taxonomical explanations of the entire radiolarian assemblages a limited number of scanning electron micrographs (SEM) and transmission electron micrographs (TEM) for the phaeodarian morphology were published in the earlier works (TAKAHASHI *et al*., 1983; TAKAHASHI, 1991). Several illustrations for fossil polycystines were provided by HURD *et al*. (1981) and partially in HURD (1983); they can be contrasted with the phaeodarians that are illustrated in this paper. Here we describe selected phaeodarian morphological characters using SEM and TEM photomicrographs up to x100,000 magnification.

Manuscript received on 25 October 2006; accepted on 7 December 2006
* Department of Earth & Planetary Sciences, Graduate School of Sciences, Kyushu University, Hakozaki 6-10-1, Higashi-ku, Fukuoka 812-8581, JAPAN; kozo@geo.kyushu-u.ac.jp
** 1626 Kinoole Street, Hilo, Hawaii 96720 USA

2. Materials and Methods

The samples employed here are mainly obtained by the PARFLUX sediment trap project (HONJO *et al.*, 1982; Table 1; Fig. 1). Several samples other than trap samples were also employed: a plankton tow sample (0-100 m verical) obtained at the Panama Basin trap station, which represents live specimens, and Core EN32PC1 from the Orca Basin of the Gulf of Mexico (BRUNNER, 1979; Table 1; Fig. 1).

Table 1. Logistics of the samples employed: PARFLUX sediment trap stations, plankton tow, and Core EN32PC1.

Trap location Geographic area	Station E Equatorial Atlantic	Station P_1 Equatorial Pacific	Station PB Panama Basin
Coordinate	13°30.2'N, 54°00.1'W	15°21.1'N, 151°28.5'W	5°21'N, 81°53'W
Trap depth (m)	389, 988, 3755	378, 978, 2778, 4280	667, 1268, 2869, 3769, 3791
Water depth (m)	5288	5792	3856
Sampled period	Nov.1977-Feb.1978	July1978-Nov.1978	Aug.1979-Dec.1979
Duration (d)	98	61	112
Sample PB 0-100 m: a plankton net was towed vertically at trap Station PB listed above in 1979.			
Piston Core location	EN32PC1 (Orca Basin, Gulf of Mexico)		
Coordinate	26°54.6'N, 91°20.5'W,		
Water depth (m)	2415		
Cored date	Jan.1979		
Core length (m)	11.73		

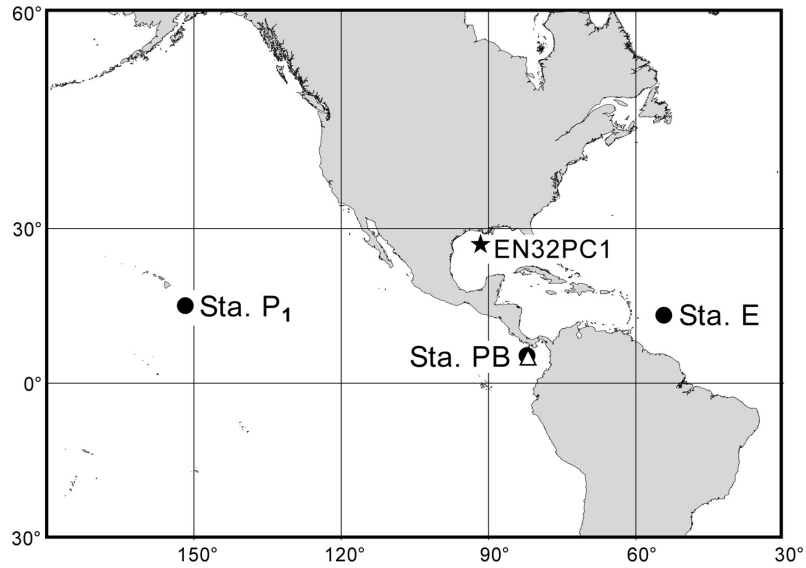

Fig. 1. Map showing the sample locations: sediment trap locations, designated by filled circles, are Stations P_1, PB, and E and a core station, denoted by a star, is EN32PC1. Station PB also includes a plankton tow sample (0-100 m verical: open triangle).

The method employed here follows those of HURD *et al*. (1981) and TAKAHASHI (1991). Briefly, phaeodarian radiolarians in sediment traps and other samples were hand picked under a stereo microscope and prepared for SEM and TEM. Prior to further processing, some specimens were ashed in an electric furnace at 500˚C for three hours to see any change in morphology due to the possible presence of organic matter in the skeletons; in this case, the photomicrographs using the ashed samples were so designated in the plate captions. For the TEM, hand picked specimens were imbedded in 2-mm-square, 1-mm-thick chips of methylene blue stained Noble agar, then dehydrated with a series of alcohol dilutions. The chips were then soaked overnight in propylene oxide and imbedded in Spurr resin. With a diamond knife approximately 500Å thick sections were taken out, put on a 300 mesh grid, and photographed at 80 to 100KEV using a Phillips 300 transmission electron microscope.

3. Discussion

It is clear that all of the phaeodarians observed here have intricately porous skeletons (Plates 2-16) compared with those of solid polycystine skeletons (Plate 1). The types of micro scale pores vary significantly from one taxonomic group to the other. For instance, the taxa belonging to Family Challengeriidae typically present “amphorae-like” pores (ancient Greek wine bottles) in a single layer (Plates 2-4) whereas those belonging to Family Medusettidae present globular pores in multiple layers (Plates 5-6). Nevertheless, the fundamental skeletal features are made of tubular units which seem to be very similar for all of the taxa examined here. The magnified views of typical tubular features are as follows: Plate 4, fig, 3; Plate 6, figs. 3-4; Plate 9, figs. 4-5; Plate 10, fig. 4, Plate 11, figs. 2, 4; Plate 12, figs. 5-6; Plate 13, fig 6; Plate 14, figs. 4-5; Plate 15, figs. 4-5; Plate 16, figs. 3-4. When a tube is cut across the tubular axis a circle is shown, whereas when a tube is cut along the axis an elongated empty line is presented (e.g., Plate 9, fig. 4; Plate 11, fig. 4; Plate 16, fig. 4). The readers can go through the series of SEM and TEM illustrations and feel the general porous morphology of phaeodarian skeletons, especially compared with those of polycystines.

One of the important features that must be noted here is the progressive change in phaeodarian morphology as a result of dissolution. Other than the porous phaedarian skeletal micro-structures such as amphorae, the remainder of the skeletons from plankton tows is relatively solid such as those presented in Plate 11, fig. 1 and TAKAHASHI *et al*. (1983). Note that the primary feature of a relatively solid unit having ca. 150-900Å pores in this fresh sample of *Castanidium longispinum* is angular. Such angular small pores were not recognized in polycystines (Plate 1), which explains their preservation in geologic record. *Gazelletta* sp. was obtained from a plankton tow (0-100 m vertical) performed in the Panama Basin illustrated in Plate 16. This specimen provides a general idea of what intact skeletons with a very thin skeletal layer look like. This fresh plankton specimen is considered to present the original skeletal morphology prior to the dissolution process which eventually alters the morphology. The tubular feature, which is only visible in partially dissolved specimens from sediment trap samples for all other taxa examined here, can already be seen in this fresh, thin, and delicate specimen. This might be a characteristic of this particular taxon. However, it is necessary to examine additional specimens/species of comparable morphology and conditions in order to make a definite conclusive remark.

Most of the skeletons presented here are from sediment traps and are thus partially dissolved. This is due to traps capturing sinking particles which were generated at the depth above the moored traps. Thus, normally the sinking time ranges from days to weeks depending on the depth interval from the production source of the particles to the trap depth. For example, based on the differential arrival of the sinking particles at two or more trap depths one can decipher the number of days for

particles spent *en route* to the traps. The amount of time spent in transit between the traps can be translated as sinking speeds. Available sinking speeds in the literature generally fall within a range from approximately 40 to 200 m d^{-1}. For example, at the pelagic subartic Pacfic Station PAPA in the Gulf of Alaska where diatoms were the major constituents of the sinking particles, the sinking speeds were estimated to be approximately 175 m d^{-1}(TAKAHASHI, 1986, 1989). In the eutrophic hemipelagic Black Sea the sinking speeds of 65±22 m d^{-1} were derived for calcium carbonate and biogenic opal (HONJO *et al*., 1987), whereas >60 m d^{-1} was observed for shell bearing plankton groups except for total diatoms of 38±18 m d^{-1} in the same set of samples (OSAWA *et al*., 2005). In addition to the transit time, the arrived particles in the trap sample containers spent some time prior to the trap recovery to a ship. After the recovery and prior to the proceeding of SEM and TEM examinations, the samples were stored in a refrigerator in the shore laboratory. Thus, the total duration of weeks to months and sometimes longer must be accounted for in the morphology observed herein.

The morphology of the observed phaeodarian skeletons shows the results of different degrees of dissolution. In addition several specimens are from the bottom sediments of the Orca Basin in the Gulf of Mexico where super brine waters provided excellent preservation of phaeodarian skeletons: *Medusetta inflata*, Plate 7. figs. 5-7; *Conchidium caudatum*, Plate 14, fig. 1.

Ashed and non-ashed specimens did not show any obvious differences (TAKAHASHI *et al*., 1983). While there were reports that phaeodarian skeletons were composed of admixtures of organic matter and silica (HAECKEL, 1887), the above observation does not support such admixtures. It is possible that the earlier workers including Earnst Haeckel saw blackened bodies of phaeodarian skeletons without identifying what part was black. Since the amphorae-like skeletal void space can be filled with organic matter while the phaeodarian lived, it is possible that such amphoral surface can become black when heated. The observation made here did not show evidence of the presence of organic matter within the skeletal structure.

4. Acknowledgements

A draft of this paper was critically reviewed by Prof. Akihiko Matsukuma of the Kyushu University Museum, for which we thank. We are grateful to Dr. Jonaotaro Onodera and Mr. Yoshiyuki Ishitani of the Kyushu University for their technical assistance in scanning of the plates. We thank E. Sarah Takahashi of the USC for techinical editing of the manuscript. This work was supported by the following research programs: MEXT Grants-in-Aid-for Scientific Research B2 Project No. 15310001 and JSPS B Project No. 17310009.

5. References

ANDERSON, O. R., NIGRINI, C., BOLTOVSKOY, D., TAKAHASHI, K., and SWANBERG, N. R. (2002) Class Polycystina. *In*: LEE, J.J., LEEDALE, G.F., and BTANDBURY, P. (eds.), *The Second Illustrated Guide to the Protozoa*, Society of Protozoologists, Lawrence, KS. 994-1022.

BRUNNER, C. A. (1979) Cruise Report: Geological and chemical investigations in the Gulf of Mexico, R/V Endeavor Cruise 32, 8 pp. [http://www.gso.uri.edu/MGSLsite/cruiserptscore.htm]

HAECKEL, E. (1887) Report on the Radiolaria collected by H.M.S."Challenger" during the years 1873-1876. *Rept. Voy*. "*Challenger*", Zool., **18**, 1-1803.

HONJO, S., MANGANINI, S.J., and POPPE, L.J. (1982) Sedimentation of lithogenic particles in the deep ocean. *Mar. Geol*., **50**, 199-220.

HONJO, S., HAY, B.J., MANGANINI, S.J., ASPER, V.L., DEGENS, E.T., KEMPE, S., ITTEKKOT, V., IZDAR,

E., KONUK, Y.T., and BENLI, H.A. (1987) Seasonal cyclicity of lithogenic particle fluxes at a southern Black Sea sediment trap station. *In*: DEGENS, E.T., IZDAR, E., HONJO , S. (eds.), *Particle flux in the ocean*, SCOPE/UNEP Sonderband Heft **62**, Mitteilungen des Geologisch-Paläontologischen Institutes, Universität Hamburg, pp. 19-39.

HURD, D. C. (1983) Physical and chemical properties of siliceous skeletons. *In*: S. R. ASTON (eds.), *Silicon Geochemistry and Biogeochemistry*, Academic Press, London, UK., 187-244.

HURD, D. C, PANKRATZ, H.S., ASPER, V., FUGATE, J., and MORROW, H. (1981) Changes in the physical and chemical properties of biogenic silica from the central equatorial Pacific: Part III, specific pore volume, mean pore size, and skeletal untrastructure of acid-cleaned samples. *Amer. Jour. Science*, **281**, 833-895.

HURD, D. C, and TAKAHASHI, K. (1983) On the estimation of minimum mechanical loss during an in situ biogenic silica dissolution experiment. *Marine Micropaleontology*, **7**, 441-447.

TAKAHASHI, K. (1986) Seasonal fluxes of pelagic diatoms in the subarctic Pacific, 1982-1983. *Deep-Sea Research*, **33**, 1225-1251.

TAKAHASHI, K. (1989) Silicoflagellates as productivity indicators: evidence from long temporal and spatial flux variability responding to hydrography in the northeastern Pacific. *Global Biogeochemical Cycles*, **3** (1), 43-61.

TAKAHASHI, K. (1991) Radiolaria: flux, ecology, and taxonomy in the Pacific and Atlantic. *In*: HONJO, S., (ed.), *Ocean Biocoenosis*, Series No. 3, Woods Hole Oceanographic Institution Press, 303 pp.

TAKAHASHI, K., HURD, D. C., and HONJO , S. (1983) Phaeodarian skeletons: Their role in silica transport to the deep sea. *Science*, **222** (4624), 616-618.

TAKAHASHI, K., and ANDERSON, O. R., 2002. Class Phaeodaria. *In*: LEE, J.J., LEEDALE, G.F., and BRANDBURY, P. (eds.), *The Second Illustrated Guide to the Protozoa*, Society of Protozoologists, Lawrence, KS. 981-994.

6. PLATES

Plate 1. For comparison with phaeodarians, intact and broken shells of solid polycystine Radiolaria are shown here; SEM: 1-3, 5; TEM: 4, 6. **1-2.** ***Acrosphaera murrayana*** (HAECKEL), belonging to colonial Radiolaria. **1.** Station & depth: $P_1$4280 m, scale bar=50μm (ID and numerals only hereafter). **2.** PB3769 m, 5μm. **3-4.** ***Myelastrum trinibrachium*** Takahashi, belonging to spongodiscoidal Radiolaria. **3.** PB1268 m, 500μm. **4.** PB2869 m, 0.2μm. **5-6.** ***Callimitra annae*** HAECKEL, belonging to nassellarian Radiolaria. **5**. $P_1$4280 m, 50μm. **6.** $P_1$4280 m, 0.2μm.

Plate 2. ***Challengerosium avicularia*** HAECKER, all SEM illustrations. **1.** $P_1$2778 m, 50μm, lateral view. **2.** $P_1$2778 m, 50μm, ventral view. **3.** $P_1$2778 m, 10μm, details of cross section near the oral teeth. **4.** $P_1$978 m, 5μm, surface texture showing both alveolate and smooth zones. **5.** $P_1$2778 m, 5μm, magnified view of 3. **6-7.** Cross section showing the amphoral structures. **6.** $P_1$2778 m, 5μm. **7.** $P_1$2778 m, 5μm.

Plate 3. All SEM illustrations. **1-2.** ***Challengeron lingi*** TAKAHASHI. **1.** $P_1$378m, 50μm. **2.** PB2869m, 5μm, details of surface texture with a small aperture located in the middle of shell wall; the presence of the aperture might well be unique to this specimen. **3-5.** *Challengeron tizardi* (MURRAY). **3.** PB1268m, 100 μm. **4.** PB1268m, 100μm, a purposely broken specimen. **5.** PB1268m, 5μm, details of the inside surface and a cross section showing amphorae. **6-9.** ***Protocystis murrayi*** (HAECKEL), an intact specimen and surface and cross sections showing the details of the amphorae. **6.** $P_1$2778m, 50μm. **7.** $P_1$2778m, 3μm. **8.** $P_1$2778m, 3μm. **9.** $P_1$2778m, 3μm.

Plate 4. ***Challengeron willemoesii*** HAECKEL, all TEM illustrations, showing various cross sections

presenting amphoral micro-structures and tubular ultra-structures. **1.** PB2869m, 5μm, ashed. **2.** PB667m, 0.1μm. **3.** PB667m, 0.2μm. **4.** PB2869m, 5μm.

Plate 5. ***Euphysetta elegans*** BORGERT, all TEM illustrations except for 1. **1.** SEM showing a whole specimen, $P_1$978m, 50μm. **2.** PB2869m, 10μm, a cross sectional micrograph across oblique transverse plane including base of large foot. **3.** PB1268m, 2μm, a cross section and inside surface of the shell. **4.** PB1268m, 2μm, a cross section and exterior of the shell. **5.** PB1268m, 2μm, an inside surface of the shell. **6.** PB1268m, 2μm, an interior the shell by intentional breakage.

Plate 6. ***Euphysetta elegans*** BORGERT, all TEM illustrations. **1.** PB2869m, 10μm, ashed. **2.** PB2869m, 2μm, ashed. **3.** PB2869m, 0.2μm, ashed. **4.** PB2869m, 0.5μm, ashed.

Plate 7. All SEM illustrations. **1-4.** ***Euphysetta lucani*** BORGERT, **1.** $P_1$978m, 100μm. **2.** E3755m, 1μm. **3.** E3755m, 1μm. **4.** E3755m, 50μm, abapical view showing a subtriangular perimeter of the shell. **5-7.** ***Medusetta inflata*** BORGERT, the same specimen, EN32PC1, 328-336 cm, **5.** 50μm, oblique abapical view. **6.** 10μm, oblique view showing the longitudinal ribs extending from the perimeter. **7.** 5μm, details of shell surface with transparent view of the skeletal interior. **8-9.** ***Medusetta ansata*** BORGERT, **8.** PB2869 m, 50μm. **9.** E389m, 2μm, broken section showing rectangular pores.

Plate 8. ***Lirella melo*** (CLEVE), SEMs (1-3, 5-6) and TEMs (4, 7). assorted views of surface textures and cross sections. **1.** PB1268m, 20μm. **2.** E3755m, 2μm. **3.** PB1268m, 50μm. **4.** PB2869m, 10μm. **5.** PB1268m, 5μm. **6.** PB1268m, 5μm. **7.** $P_1$4280m, 2μm.

Plate 9. ***Lirella melo*** (CLEVE), all TEM illustrations. Various cross sections showing polygonal meshwork and porous outer layers. Note that the polygons are made of tubes, visualized at high magnifications. **1.** $P_1$978m, 5μm. **2.** $P_1$4280m, 0.2μm. **3.** PB2869m, 1μm, ashed. **4.** $P_1$4500m, 0.2μm. **5.** PB2869m, 0.5μm, ashed.

Plate 10. ***Castanidium abuntiplanatum*** TAKAHASHI, all TEM illustrations except for 1 (SEM). **1.** PB3769m, 200μm. **2.** PB3769m, 2μm. **3.** PB3769m, 0.2μm. **4.** PB3769m, 0.2μm. **5.** *Castanella* sp., $P_1$1000m, 0.5μm. **6-7.** ***Castanidium longispinum*** HAECKER, **6.** E389m, 5μm. **7.** PB667m, 5μm.

Plate 11. ***Castanidium longispinum*** HAECKER, all TEM illustrations. **1.** PB 0-100m plankton tow, 0.5μm, primary feature of relatively solid unit having ca. 150-900Å pores; conchoidal fractures are artifact with the sectioning. **2.** PB1268m, 0.5μm. **3.** PB1268m, 5μm. **4.** PB1268m, 0.5μm.

Plate 12. 1-6. ***Haeckeliana porcellana*** MURRAY, all TEM illustrations except for 1-2 (SEMs). **1.** E988m, 100μm. **2.** $P_1$978 m, 5μm. **3.** $P_1$978m, 5μm. **4.** $P_1$978m, 5μm. **5.** $P_1$978m, 0.5μm. **6.** $P_1$978m, 0.5μm.

Plate 13. 1-6. ***Conchellium capsula*** BORGERT, all TEM illustrations except for 1, 3 (SEMs). **1.** E389m, 50μm. **2.** $P_1$2778m, 1μm, relatively undissolved specimen with the outermost thin porous layer. **3.** E3755m, 2μm, partially dissolved specimen showing the thin solid outer layer covering the porous inner layer. **4.** $P_1$2778m, 1μm, partially dissolved interior and still intact relatively solid skeleton. **5.** E3755m, 1μm, cross section showing relatively solid portions, porous layer, and the relatively solid external layer. **6.** $P_1$2778m, 0.1μm, magnified details for the external layer and the subinterior underneath.

Plate 14. ***Conchidium caudatum*** (HAECKEL), all TEM illustrations except for 1, 3 (SEMs). **1.** EN32PC1, 744-756cm, 100μm. **2.** $P_1$2778m, 0.5μm. **3.** E389m, 10μm. **4.** $P_1$2778m, 0.5μm. **5.** $P_1$2778m, 0.1μm. **6.** $P_1$2778m, 0.5μm.

Plate 15. ***Conchidium argiope*** HAECKEL, all TEM illustrations except for 1 (SEM). **1.** EN32PC1, 744-756cm, 50μm. **2.** PB1268m, 1μm. **3.** PB3791m, 1μm. **4.** PB1268m, 0.5μm. **5.** PB1268m, 0.5μm, ashed.

Plate 16. 1-4. ***Gazelletta*** **sp.**, all TEM illustrations, the same specimen, PB 0-100 m plankton tow. Note that the taxonomic labels presented in TAKAHASHI (1991: *Medusetta* sp. B) is revised herein. **1.** 2μm. **2.** 10μm. **3.** 0.5μm. **4.** 0.1μm, basic structure made of tubular units.

Plate 1

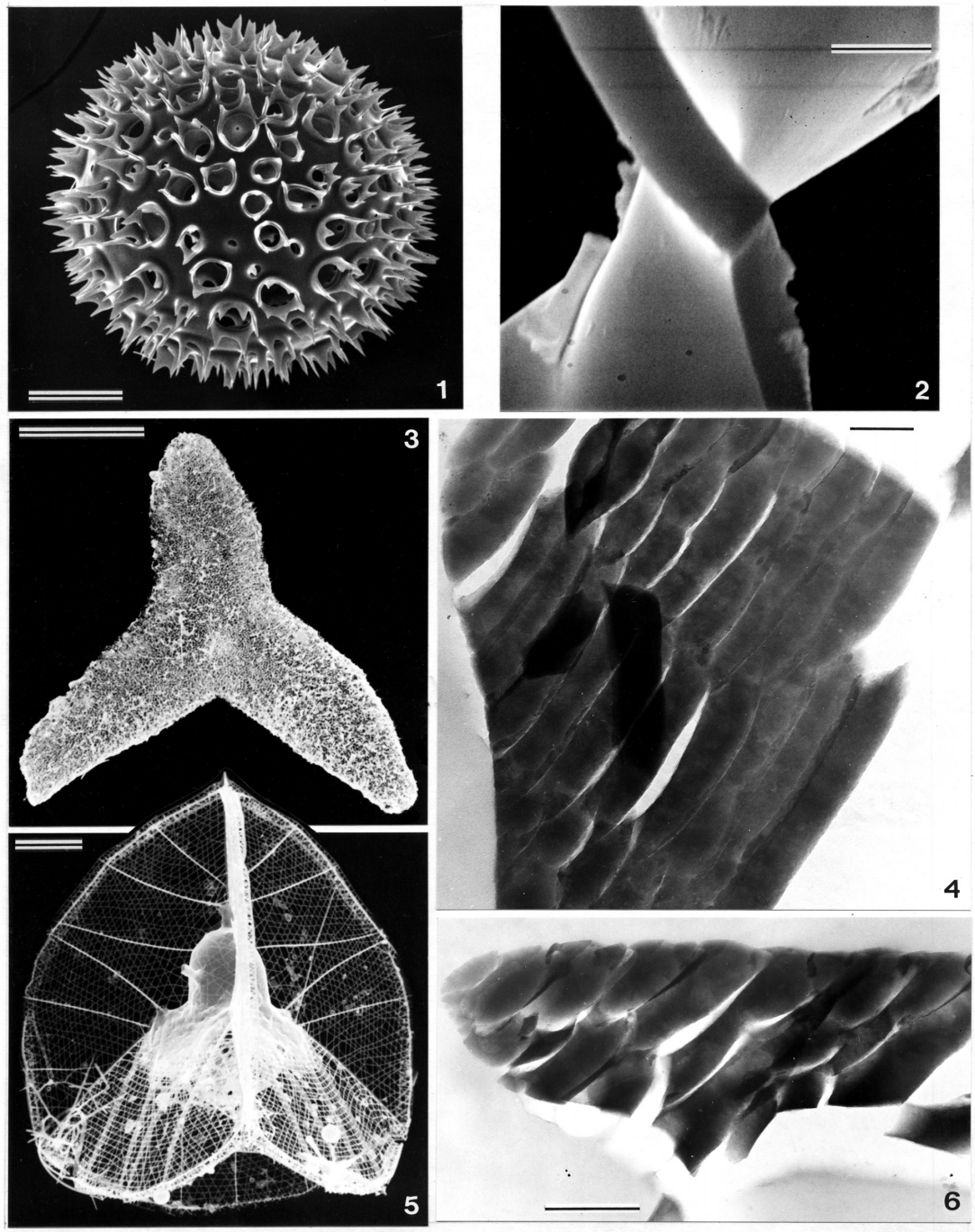

Plate 2

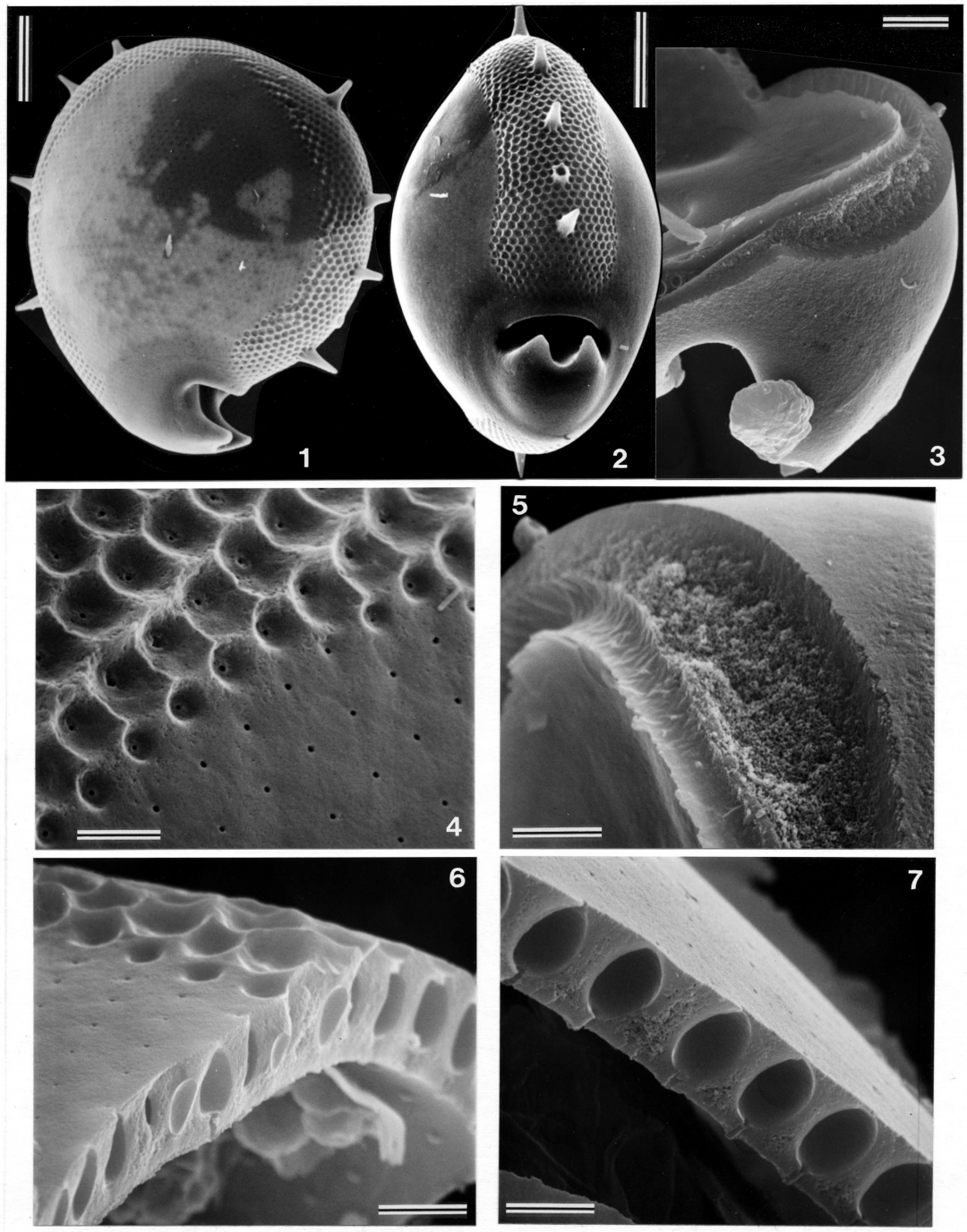

Plate 3

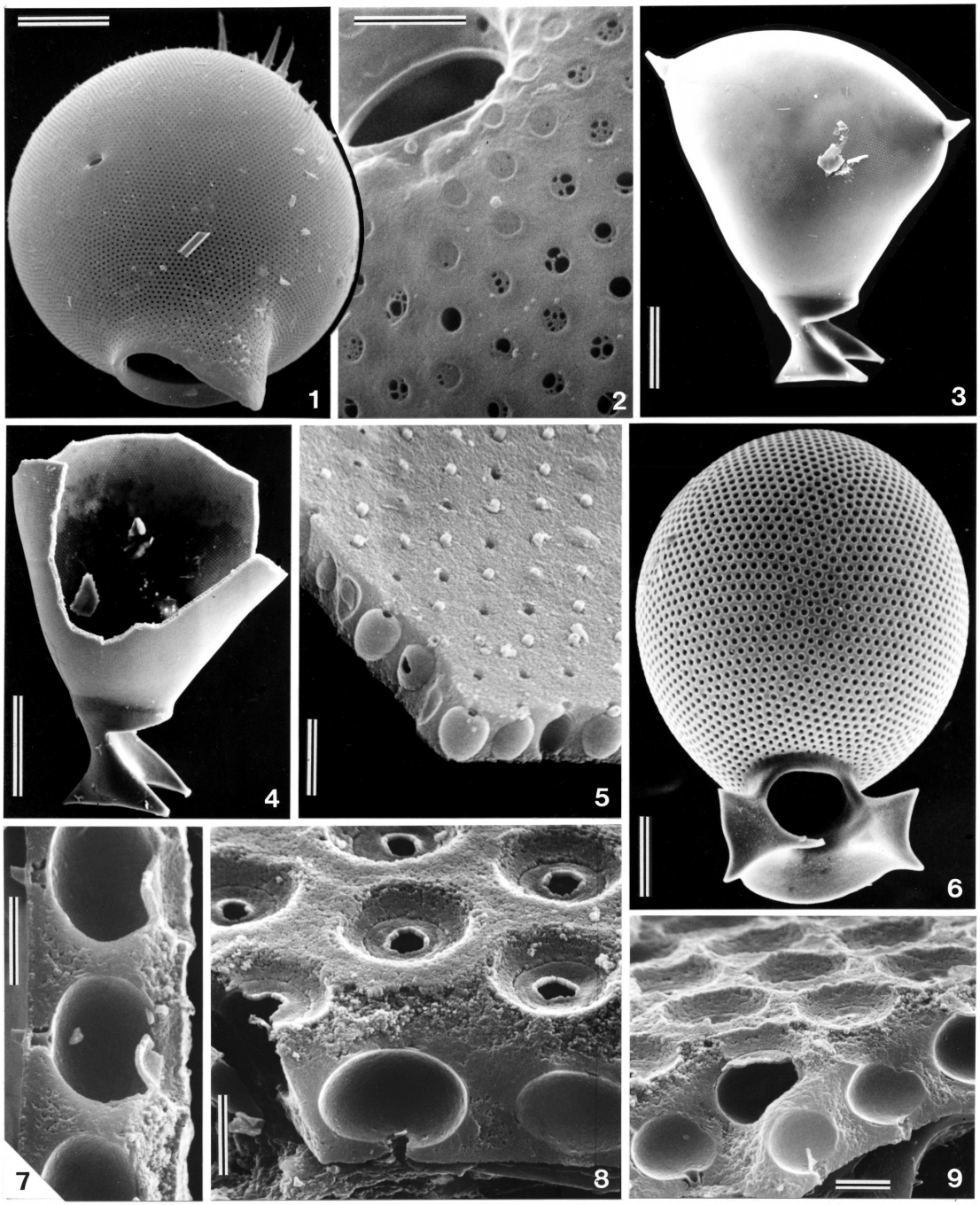

Plate 4

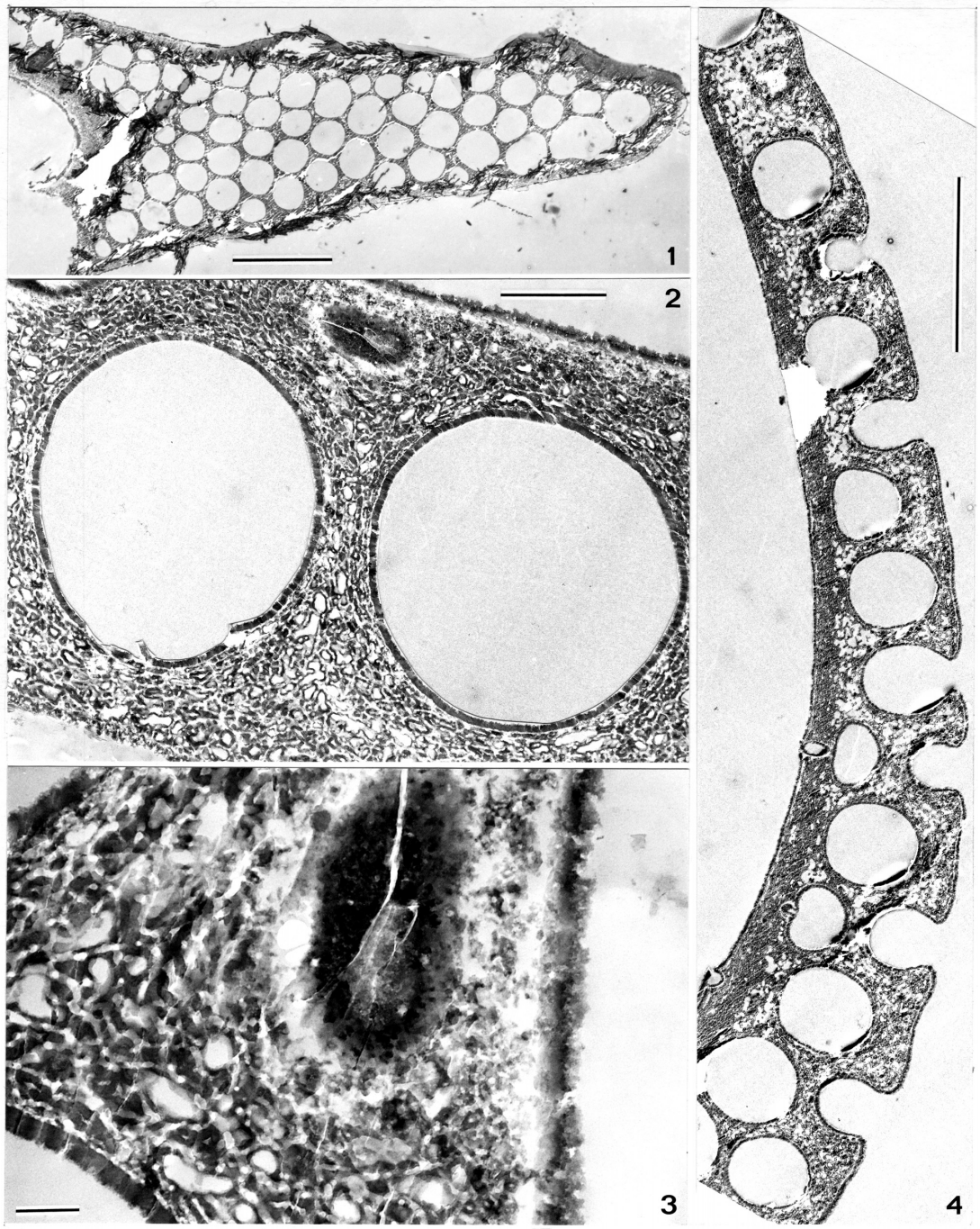

Plate 5

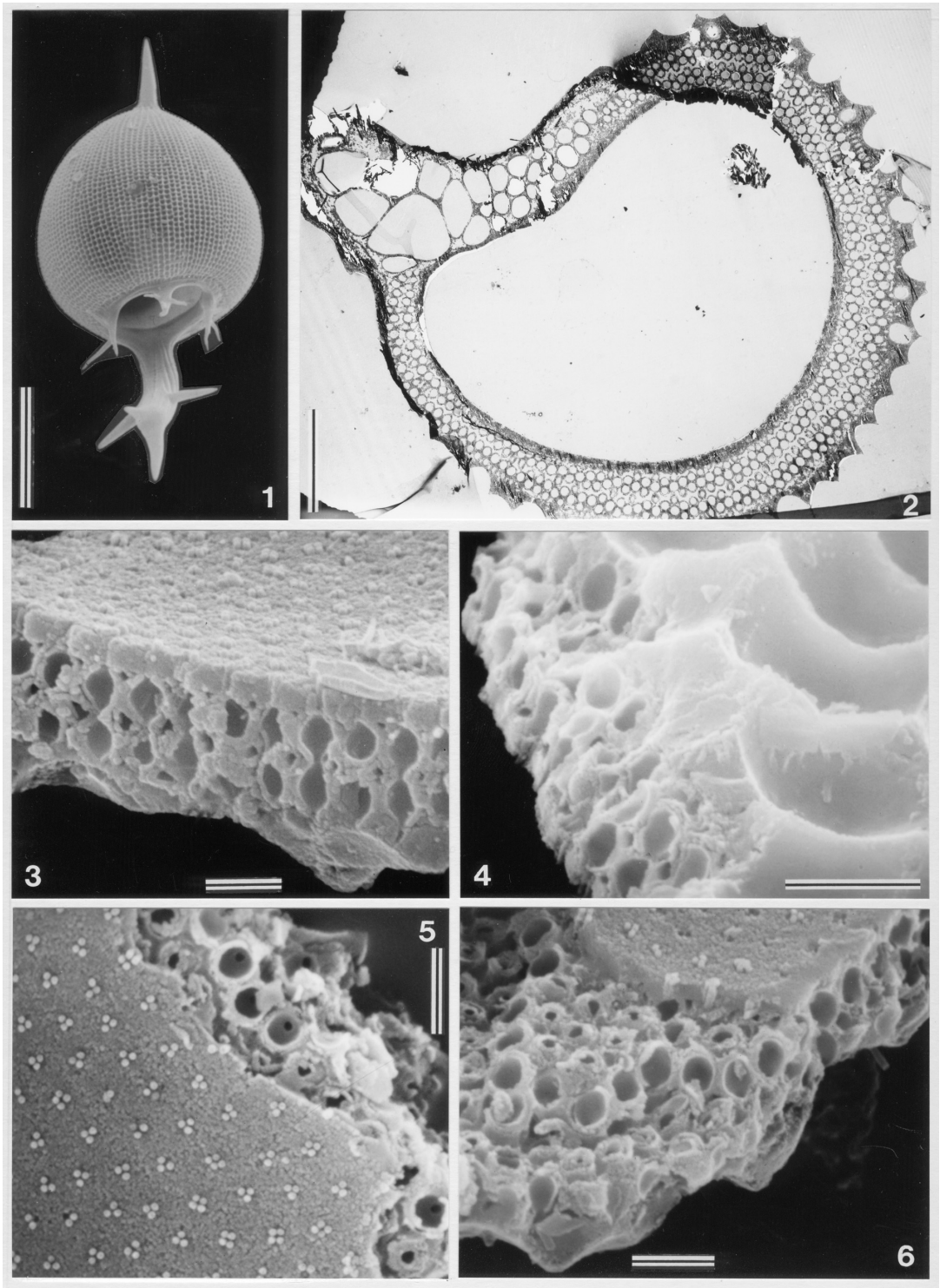

Plate 6

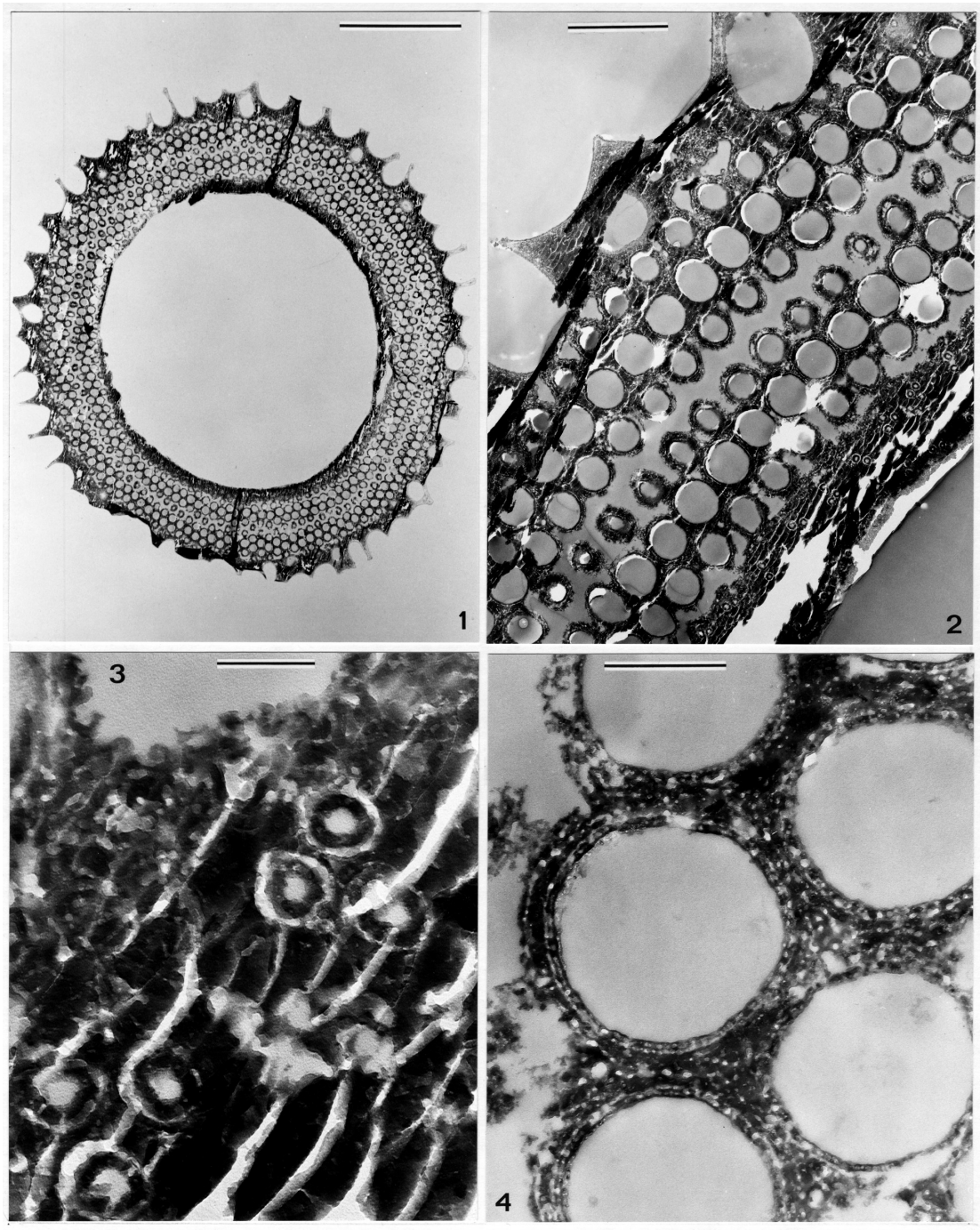

Plate 7

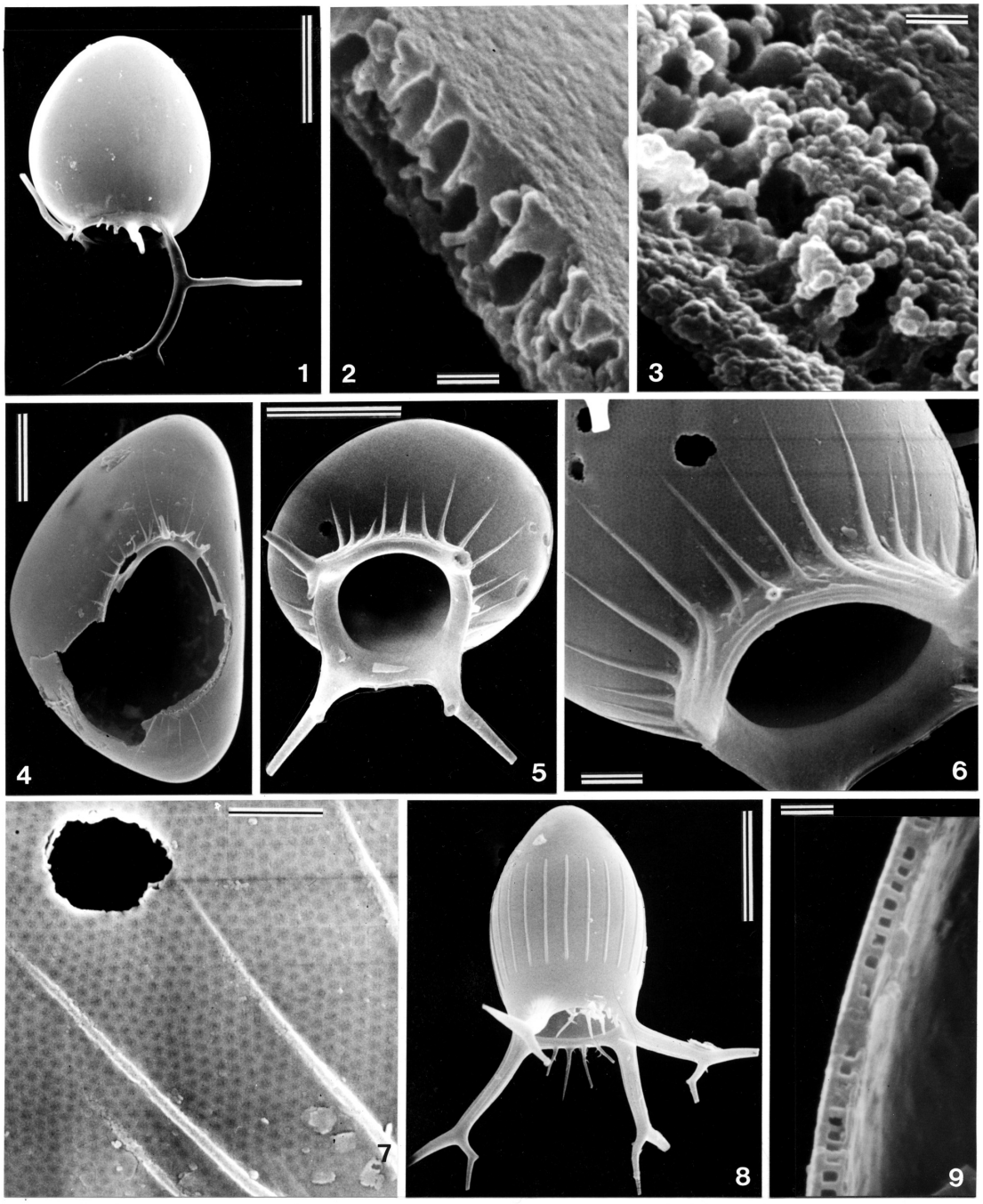

Plate 8

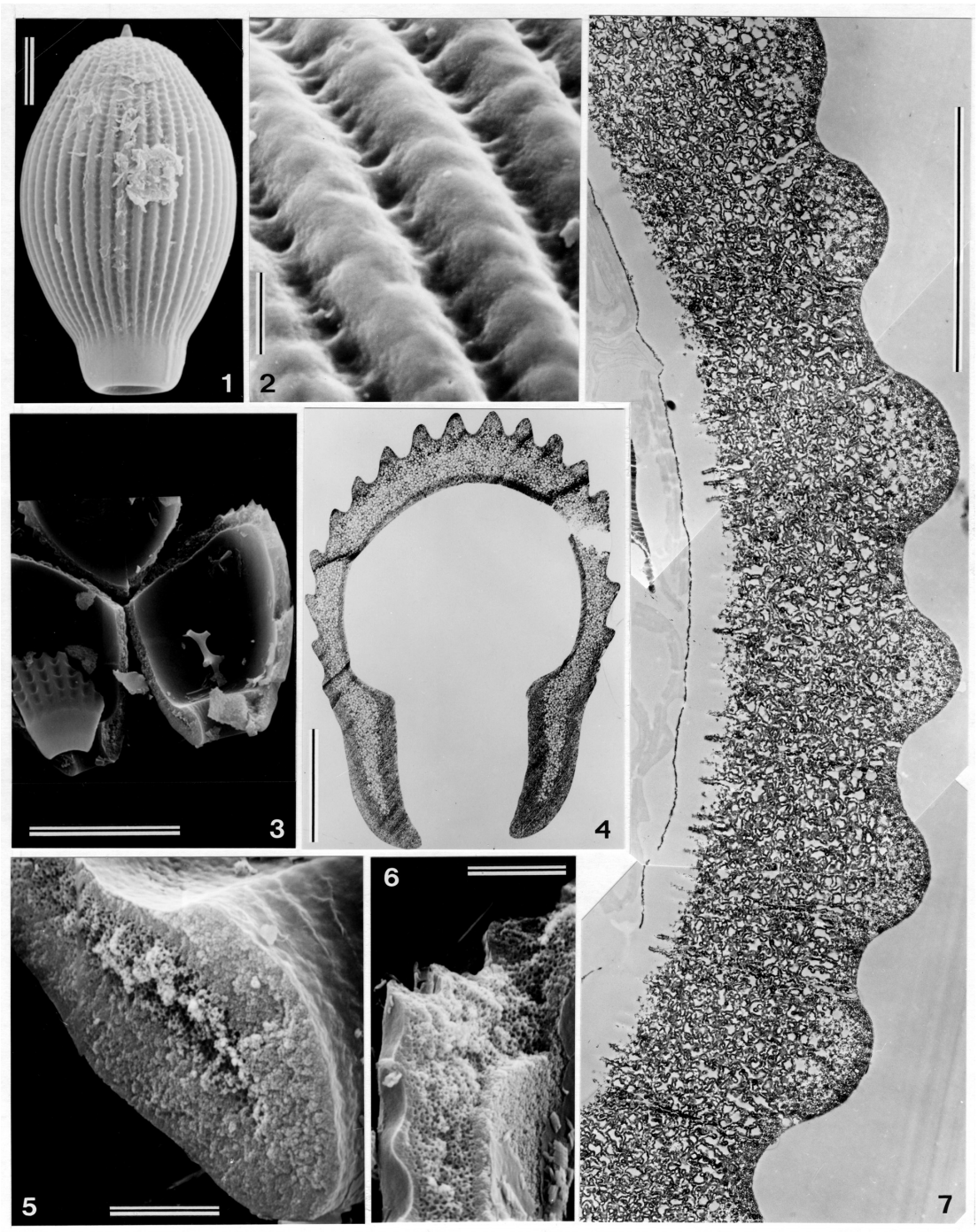

Plate 9

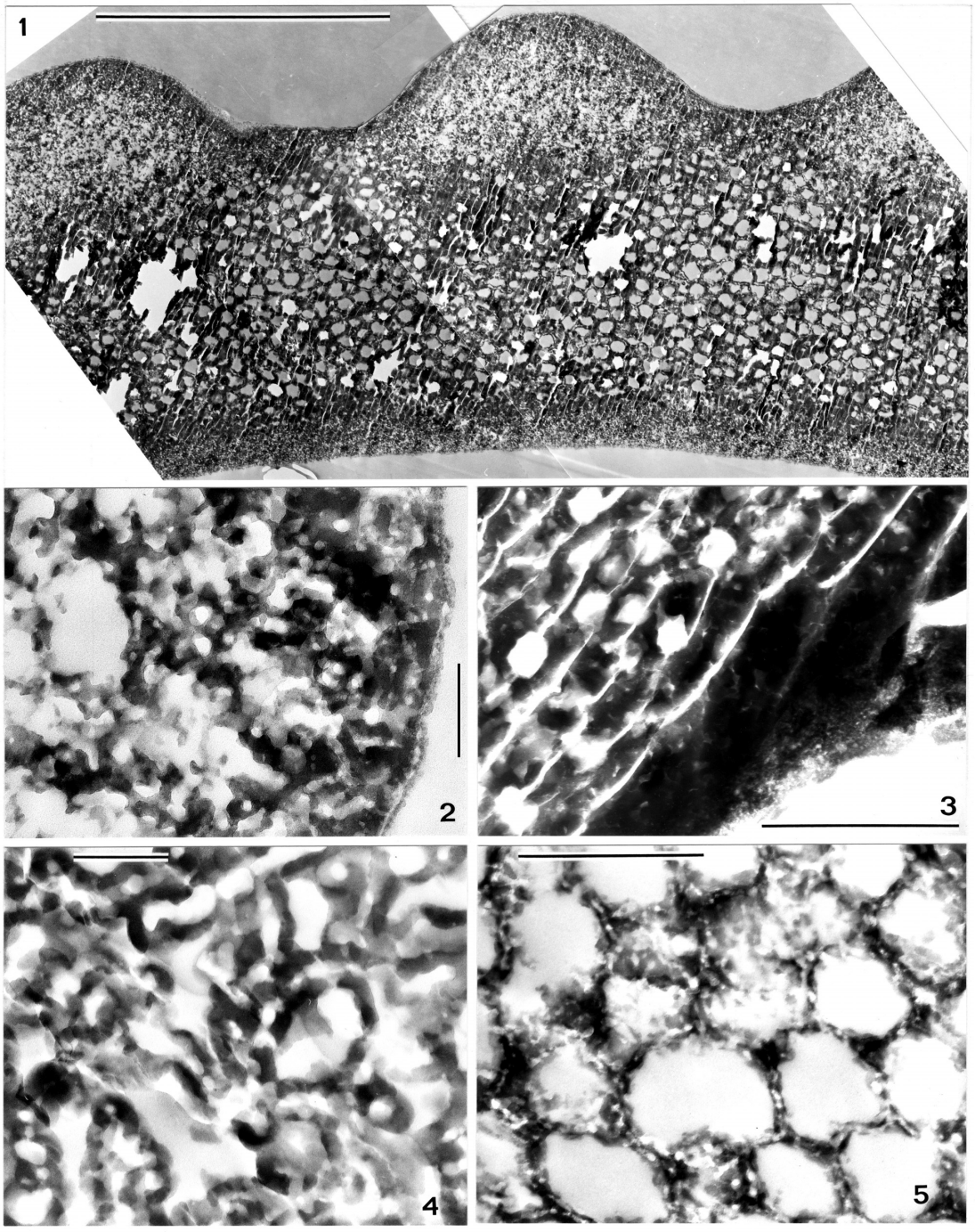

Plate 10

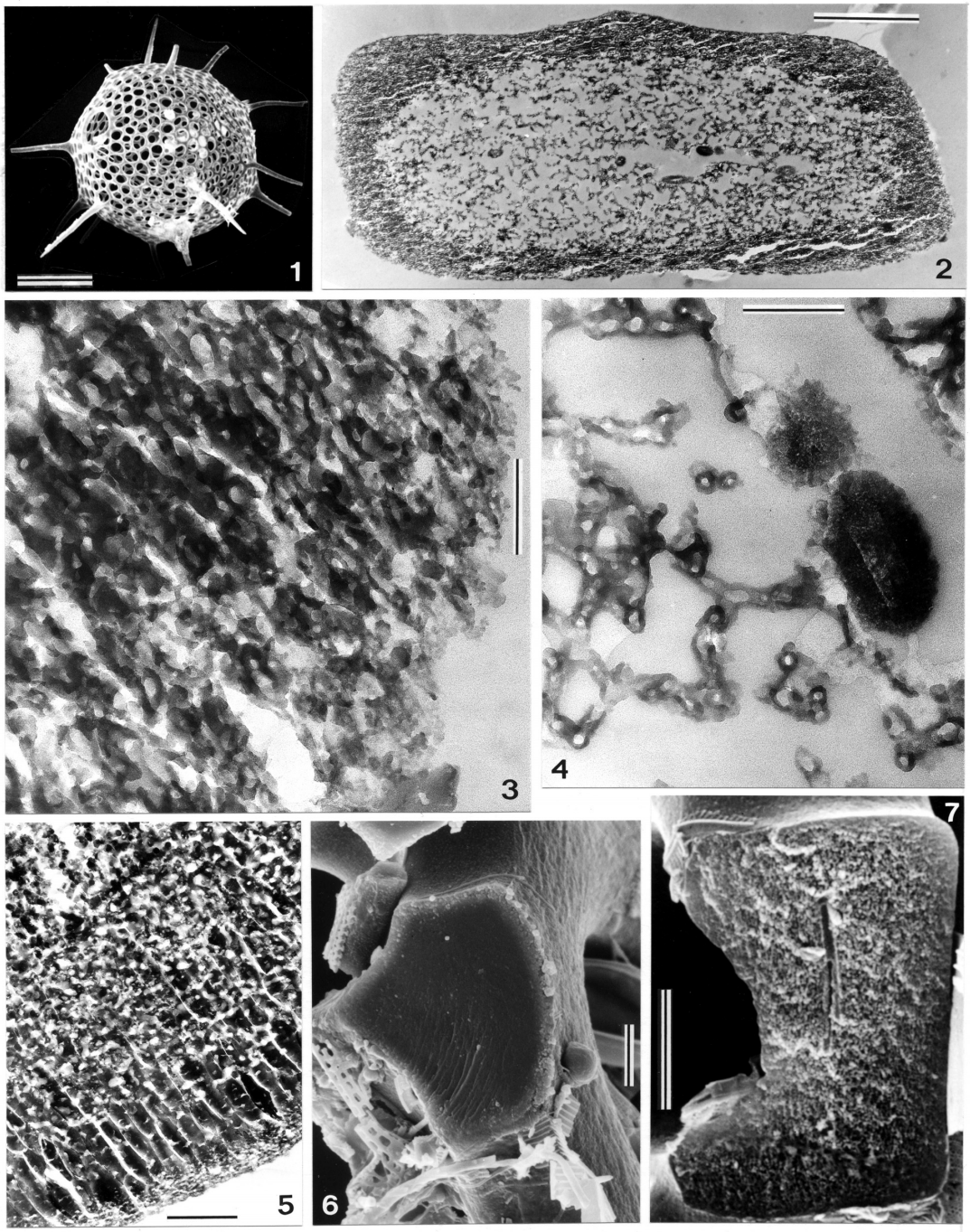

Plate 11

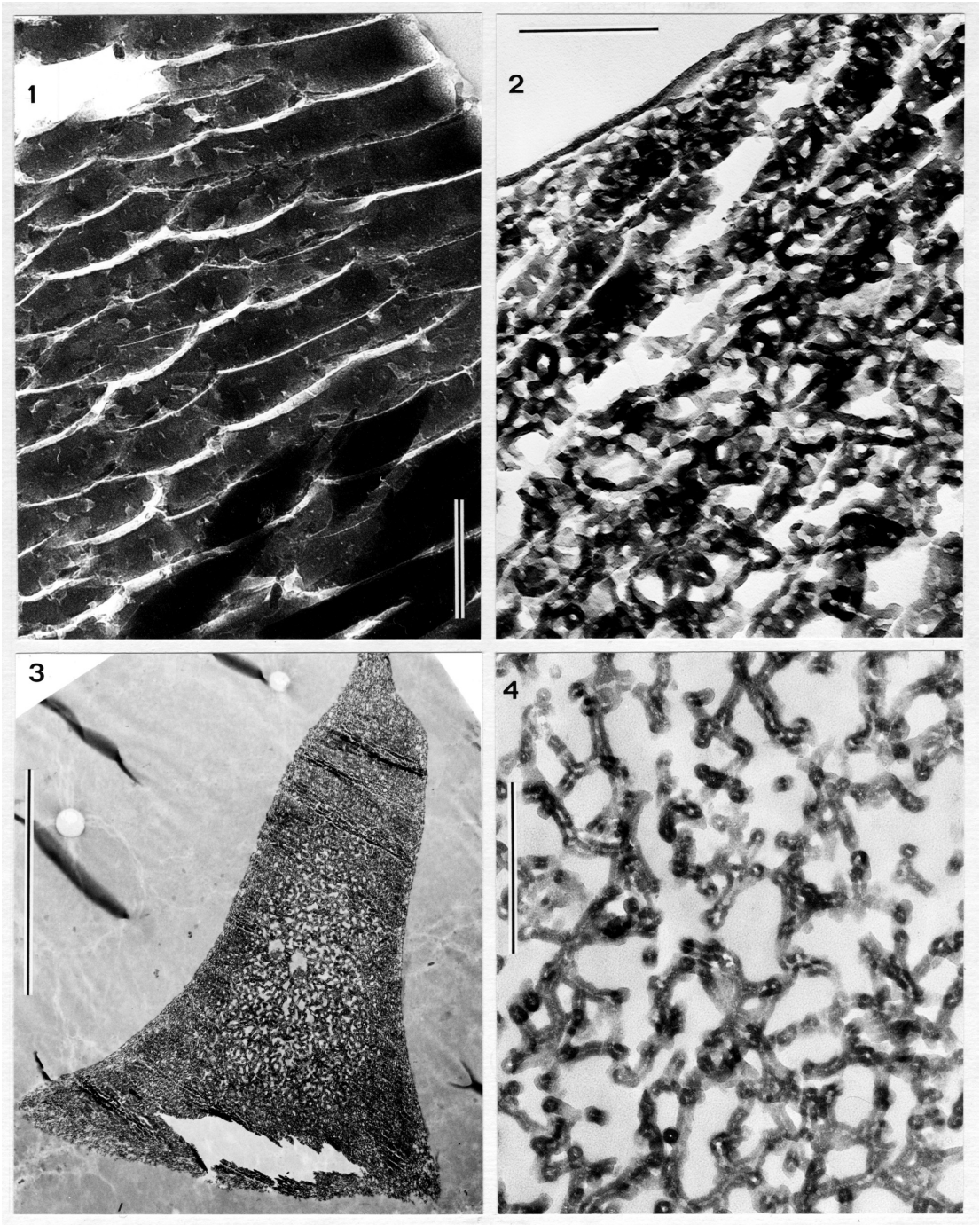

Plate 12

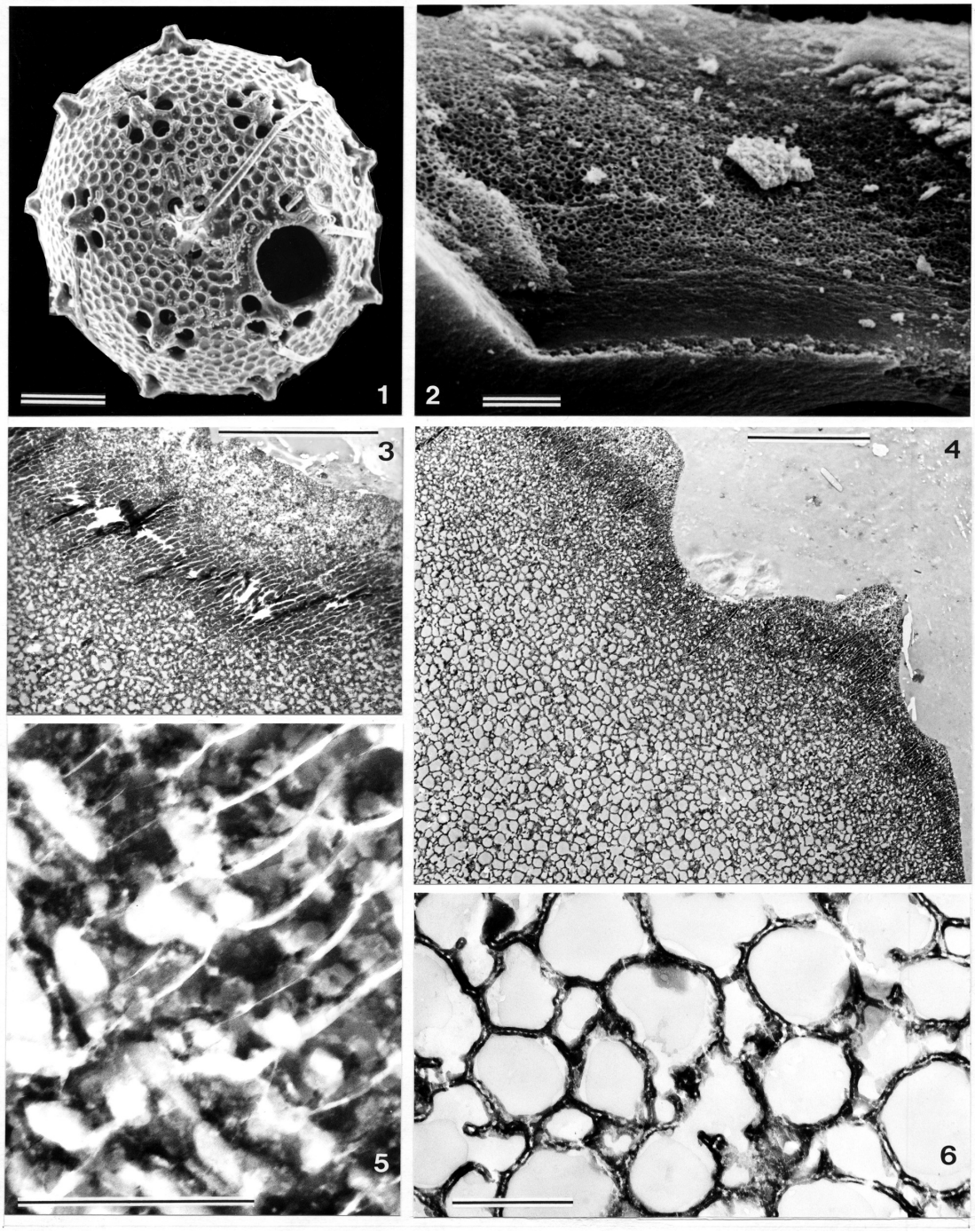

Plate 13

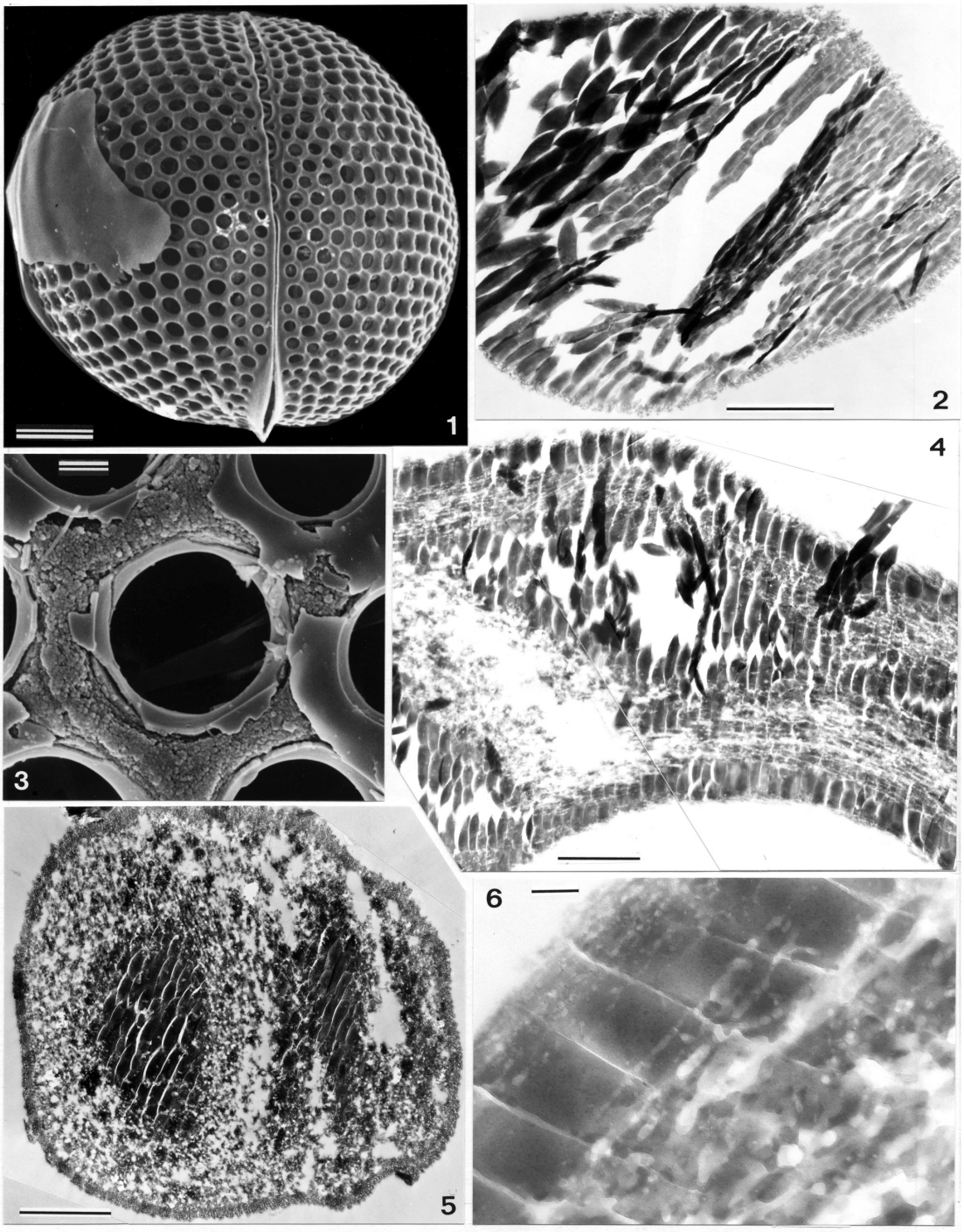

Plate 14

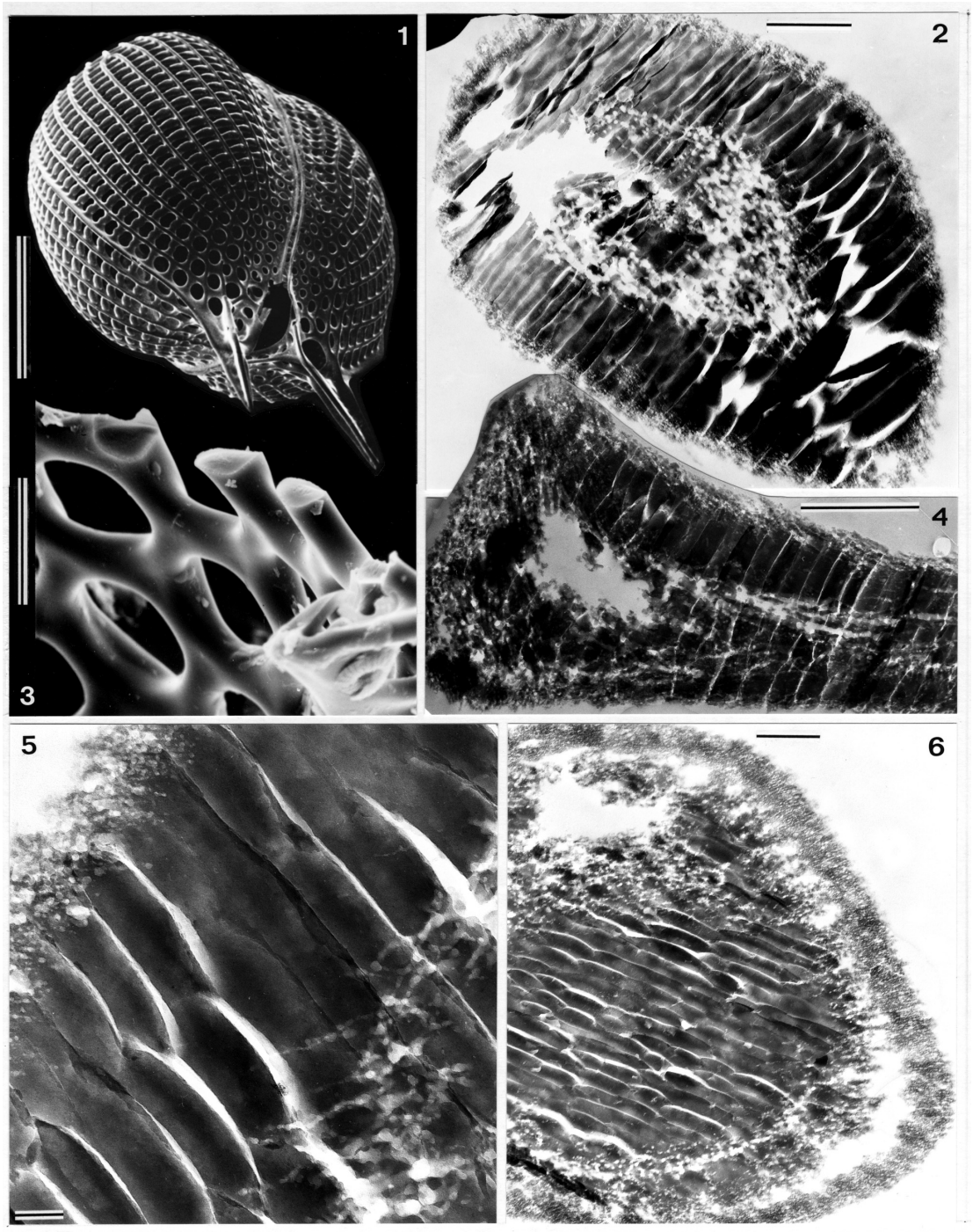

Plate 15

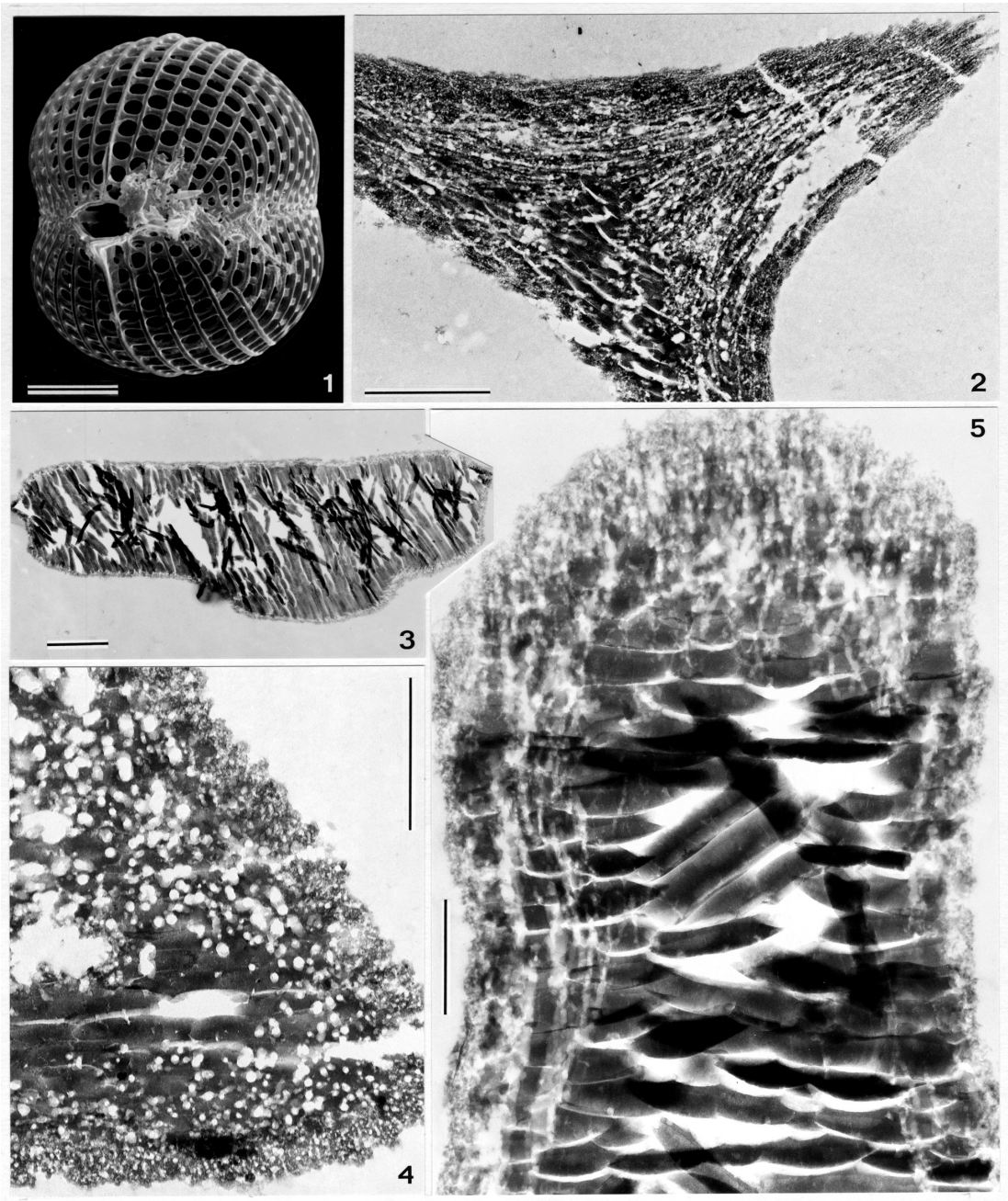

Plate 16